International Journal for Housing Science and Its Applications
Publish August 4, 2025. Volume 46, Issue 3 Pages 2798-2811

https://doi.org/10.70517/ijhsa463235

A Method for Unmanned Construction Machine Fleet Collaborative Operation and Road Safety Assurance Based on Optimal Control

Lihu Pei[1] and Dushan Ma[1,*]
[1] Gansu Wan Tai Construction Group, Lanzhou, Gansu, 730000, China
Corresponding authors: (e-mail: dushanbridge@163.com).

Abstract In order to improve the quality of UAV application in highway pavement construction, the study firstly establishes the mathematical model and formation model of pavement construction UAV. Then a path planning algorithm based on improved RAPA is designed, which optimizes the search process by combining the jump point search algorithm. And the loopback force is introduced into the artificial potential field method to improve the local minimum problem, which is applied in planning path and obstacle avoidance. Finally, the sliding mode path tracking control law is designed for the motion model and attitude model of the pavement construction UAV respectively to ensure the accurate tracking of the construction path by the pavement construction UAV formation. The study is simulated and verified in MatlabR2018a, and the three UAVs are able to ensure smooth obstacle avoidance with smooth paths, continue to track the target effectively, and maintain a safe distance of more than 100m from all obstacles. The engineering application results of 8 pavement construction UAVs show that the proposed path planning method can carry out the pavement construction path planning in each material area, and the unmanned milling machine fleet can automatically avoid obstacles and guarantee the milling efficiency during the operation. In order to further guarantee the construction safety, the application effect of unmanned machine is improved through the measures of selecting the best unmanned machine equipment, making good planning and designing of aerial photography operation, making good use of the results of aerial photography, and enhancing the integration of technology and other means.

Index Terms Formation model, path planning algorithm, jump point search algorithm, pavement construction

I. Introduction

Nowadays, engineering projects gradually tend to scale, complexity and internationalization, and the intensity of information communication and dissemination has increased dramatically, leading to the expansion of the demand for construction information management [1], [2]. Taking highway construction projects as an example, with the gradual expansion of the scope of highway construction, the number of highways constructed in mountainous areas or areas with peculiar geomorphology is also increasing [3], [4]. Due to the complex geological conditions in these areas, the speed of highway construction is inhibited, the difficulty of highway construction is increased, and the life safety of construction personnel is also threatened [5]. In the face of the complex and changeable construction information management problems, the traditional management method has been difficult to meet the actual engineering needs due to its inefficient information acquisition, lack of data resources, insufficient safety and security, and susceptibility to personal subjective judgment [6]-[8]. Therefore, by adopting cutting-edge information integration technology, exploring the construction of a high-efficiency project information management system for the unique information management requirements and the latest technical solutions in the field of building construction is the core strategy to break through the current difficulties in construction project management [9]-[11].

With the continuous evolution of society and the continuous innovation of science and technology, UAV near-ground remote sensing technology has become a research hotspot because of its excellent performance and wide application prospects. This technology mainly collects the three-dimensional spatial position, geometric shape, radiation characteristics and spectral information of the target to realize accurate positioning and efficient data collection, using unmanned aerial vehicle as a mobile platform and integrating advanced sensors, such as high-precision visible camera and thermal infrared camera, to ensure comprehensive and omission-free acquisition of images [12]-[15]. The application of UAV technology in highway pavement construction projects substantially improves the construction efficiency and accuracy, and plays a central role in transportation fields such as highway construction and operation and maintenance information control [16]-[18].

In this paper, after establishing the pavement construction UAV formation model, we explore the path planning and control methods for the cooperative operation of UAVs. A path planning algorithm based on improved RAPA is designed, which optimizes the search process by preprocessing obstacle information and combining the jump point search strategy. After that, the motion loop sliding mode control law and attitude loop sliding mode control law are designed to ensure the UAV's accurate tracking of the desired path output from the improved artificial potential field method. The application effect of the designed path planning and control method is verified through simulation tests and practical applications. In addition, the study proposes relevant protection strategies for the safety of UAVs in highway pavement construction.

II. Modeling

This chapter establishes a mathematical model of pavement construction UAVs, based on the premise to realize the quality improvement research of unmanned swarms in highway pavement construction.

II. A.Establishment of a mathematical model for pavement construction UAVs

The motion model of the road construction UAV is shown in equation (1):

$$\begin{cases} \dot{p} = v \\ \dot{v} = -G + hT \end{cases} \tag{1}$$

where, p - the trajectory of the UAV, $p=\left[x,\ y,\ z\right]^T$, m, v - the speed of the drone's motion, $v=\left[v_x,\ v_y,\ v_z\right]^T$, m/s, G -acceleration of the drone, $G=\left[g_x,\ g_y,\ g_z\right]^T$, m/s^2, T - the lift generated by the drone, $T=\left[T_x,T_y,T_z\right]^T$, N, h - coefficient matrix of the UAV motion model:

$$h=\frac{1}{m}\begin{bmatrix} 0 & 0 & \sin\theta\cos\psi\cos\phi+\sin\psi\sin\phi \\ 0 & 0 & \sin\theta\sin\psi\cos\phi-\cos\psi\sin\phi \\ 0 & 0 & \cos\theta\cos\phi \end{bmatrix} \tag{2}$$

where, m - mass of the UAV, kg, ϕ,θ,ψ - roll, pitch and heading angles, (°), Attitude model of road construction UAV:

$$\begin{cases} \dot{\Theta}=W\omega \\ J\dot{\omega}=-\omega\times J\omega+\Gamma_0 \end{cases} \tag{3}$$

where, Θ - UAV attitude angle, $\Theta=[\phi,\theta,\psi]^T$, (°), w - UAV's roll, pitch and yaw angular velocity, $\omega=\left[p,q,r\right]^T$, (°), J - Inertia matrix of the UAV, $J=diag\left\{J_x,J_y,J_z\right\}$, Γ_0 - roll, pitch and yaw moments, $\Gamma_0=\left[\Gamma_x,\Gamma_y,\Gamma_z\right]^T$, N·m. W - coefficient matrix of the UAV attitude model:

$$W=\begin{bmatrix} 1 & \sin\phi\tan\theta & \cos\phi\tan\theta \\ 0 & \cos\phi & -\sin\phi \\ 0 & \sin\phi/\cos\theta & \cos\phi/\cos\theta \end{bmatrix} \tag{4}$$

Let $f=J^{-1}(-\omega\times J\omega),\Gamma=J^{-1}\Gamma_0$, then the attitude model of the pavement construction UAV can be deformed as:

$$\begin{cases} \dot{\omega}=W\omega \\ \dot{\omega}=f+\Gamma \end{cases} \tag{5}$$

With the construction operation, the mass of the pavement construction UAV will gradually decrease, so the motion model (1) and attitude model (5) cannot accurately describe the actual motion of the pavement construction UAV. In order to be closer to reality, a disturbance term is introduced into the pavement construction UAV, then the expressions of the motion model and attitude model of the pavement construction UAV with disturbance are shown in Eq. (6) and Eq. (7), respectively:

$$\begin{cases} \dot{p}=v \\ \dot{v}=-G+hT+d_v \end{cases} \tag{6}$$

$$\begin{cases} \dot{\Theta} = W\omega \\ \dot{\omega} = f + \Gamma + d_w \end{cases} \tag{7}$$

where, d - perturbation term for the motion model, d_a - the perturbation term of the attitude model.

II. B.Modeling UAV formations

In order to realize the cooperative operation mode of multiple pavement construction UAVs, it is necessary to carry out formation flight operations, which can greatly improve the operational efficiency, and the leader of the fleet needs to be set up in the formation, and the construction path of the leader UAV is planned according to the operational object, and the other UAVs fly after the leader [19]. The formation architecture is shown in Fig. 1. UAV_1 denotes the leader pavement construction UAV, and (x_1, y_1, z_1) is the construction path of UAV_1 obtained by the path planning algorithm. UAV_f denotes the follower pavement construction UAV, (x_f, y_f, z_f) is the construction path of UAV_f, and (x_d, y_d, z_d) is the construction path of UAV_f with UAV_1 is the expected distance between UAV_f and UAV_1.

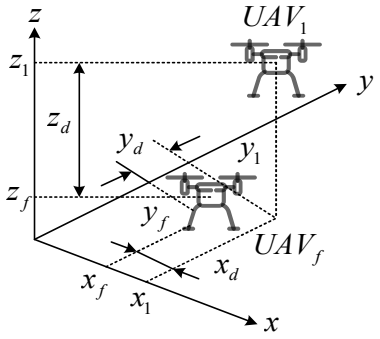

Figure 1: Schematic diagram of formation

Then the formation model of multiple pavement construction UAVs is described as:

$$\begin{cases} x_i = x_1 - 2x_c \\ y_i = y_1 - 2y_c \\ z_i = z_1 - 2z_c \end{cases} \tag{8}$$

$$U_{po}(X_p, X_o) = \begin{cases} +\infty \\ b\left[\dfrac{l(X_p, X_o)}{\rho_0^2} - \dfrac{2\ln[l(X_p, X_o)]}{\rho_0} - \dfrac{1}{l(X_p, X_o)}\right] \\ 0 \end{cases} \tag{9}$$

where, $U_{po}(X_p, X_o)$ - the repulsive force field to which the pavement construction UAV formation is subjected, $l(X_p, X_o)$ - distance of the pavement construction UAV formation from the center of the repulsive field, m, R_0 - radius of the obstacle zone, m, ρ_0 - radius of the repulsive field generated by the obstacle zone, m, b - the gain coefficient of the repulsive field.

Negative gradient operation on Eq. (9) yields the repulsive force function description of the obstacle zone as shown in Eq. (10):

$$F_{po}(X_p, X_o) = \begin{cases} +\infty & 0 \le l(X_p, X_o) < R_0 \\ b\left[\dfrac{1}{\rho_0} - \dfrac{1}{l(X_p, X_o)}\right]^2 & R_0 \le l(X_p, X_o) \le R_0 + \rho_0 \\ 0 & l(X_p, X_o) > R_0 + \rho_0 \end{cases} \tag{10}$$

In Eq, $F_{po}(X_p, X_o)$ - repulsive force on the pavement construction UAV formation, N, x_c, y_c - components of the maximum construction radius in the direction of the x-axis and y-axis for the pavement construction UAV at the height z_c.

The construction path of the follower pavement construction UAV can be obtained from equation (8).

III. Route planning and control methodology design

Based on the UAV formation model established above, this chapter provides optimal planning and control of the UAV flight path.

III. A. Improved RAPA-based path planning

III. A. 1) Improvement of RAPA path planning algorithm

In path planning, the jump point search algorithm (JPS) has certain limitations [20], in order to solve the problem of large computation and serious memory occupation caused by storing a large number of useless jump points in the planning process of the JPS algorithm, this paper proposes an improved algorithm that combines the artificial potential field method [21] with the RAPA algorithm.

The RAPA path planning algorithm is defined as follows: first, detection is carried out in the detection area, and the artificial potential field method is used for obstacle avoidance if the combined force is zero or oscillation does not occur during the UAV flight. If the combined force is zero oscillation or encounter large obstacles, or flight direction of the hemispherical plane of the Dos layer of four or more different regions at the same time obstacles, and cause the UAV can not avoid obstacles, that is, shown in equation (11):

$$F = 0 \text{ or } \sum \varepsilon(DOS) \geq 4 \tag{11}$$

The node where the current UAV is located is taken as the starting node, and the first node in the half plane $\sum \varepsilon(DOS) = 0$ of the flight direction after avoiding obstacles is taken as the termination node. Rasterize the map of the detected area and start screening the jump points and apply the improved A-star algorithm for obstacle avoidance, then the flow of the RAPA algorithm is shown in Fig. 2.

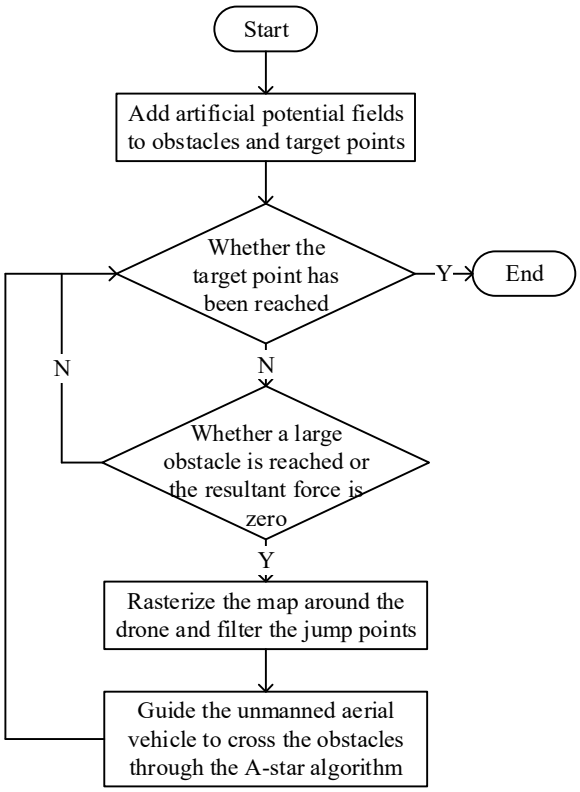

Figure 2: Flow chart of PARA algorithm

Conducting a search requires visiting 26 nodes, which will greatly increase the computational difficulty and time, so this study improves the RAPA algorithm based on the jump point search algorithm. A pre-processing process of nodes will be added on the basis of RAPA algorithm to screen out a batch of jump points in advance, which can greatly reduce the access and calculation of RAPA algorithm in a large number of intermediate and unnecessary nodes. The improved RAPA algorithm does not need to traverse all the nodes, but long-distance jumps to calculate special nodes.

The preprocessing process is essentially the process of screening the jump points in the raster map, which is defined in this paper according to the actual situation. The UAV cannot obtain the information of the whole map when it is working, but the UAV has a detection area and can obtain the localized information. For the UAV, it has not detected the obstacle A i.e. $R(A,B,C)=\begin{pmatrix}0&0&0&1\\1&1&0&1\end{pmatrix}$ when no node is set. When obstacle A is detected in the UAV detection area i.e. $R(A,B,C)=\begin{pmatrix}0&1&0&1\\1&1&0&1\end{pmatrix}$ when generalizing the local map to take out all 26 nodes around it.

Let the coordinates of the nodes be $(x_i,y_i,z_i)i=1,2\cdots 26$, the coordinates of the drone be (x_u,y_u,z_u), and the distance from the nodes to the drone, d, be $d_u i=\sqrt{(x_i-x_u)^2+(y_i-y_u)^2+(z_i-z_u)^2}$, and the unit vector of the node's direction to the drone is $\overline{V}_{wi}(x_{wi},y_{wi},z_{wi})=\left(\frac{(x_i-x_u)}{d_{wi}},\frac{(y_i-y_w)}{d_{wi}},\frac{(z_i-z_w)}{d_{wi}}\right)$. Target point coordinates (x_t,y_t,z_t). Define the line connecting the current position of the UAV to the target point as V_w, and the distance d is $d_w=\sqrt{(x_t-x_u)}^2+(y_t-y_u)^2+(z_t-z_u)^2$, and the direction unit vector is: $\overline{V}_{ut}(x_{vt},y_{vt},z_{vt})=\left(\frac{(x_t-x_u)}{d_{ui}},\frac{(y_t-y_u)}{d_{ui}},\frac{(z_t-z_u)}{d_{ui}}\right)$, and for a better filtering of the nodes, compute the unit vectors $\overline{V}_{ui}$ and $\overline{V}_{ut}$ of the inner product N, which leads to equation:

$$N=\overrightarrow{V_{ui}}\times\overrightarrow{V_{ut}}=x_{vi}\cdot x_{vt}+y_{vi}\cdot y_{vt}+z_{vi}\cdot z_{vt}\begin{cases}N>0,\text{Retain the corresponding nodes}\\N\le 0,\text{Delete the corresponding node}\end{cases}\tag{12}$$

The nodes corresponding to the inner product are retained if $N>0$, and the corresponding nodes are removed if $N\le 0$, so that a group of jump points can be further filtered.

In this paper, other nodes are regarded as unnecessary nodes, due to the fact that the moving path of RAPA algorithm is not smooth enough and there are many inflection points, which is unfavorable to the rotation and displacement of the UAV. Then after screening the jump points and determining the best moving path, the path is smoothed by using the nearest neighbor interpolation method, which is more in line with the UAV's movement pattern, as shown in equation, to reduce the difficulty of the UAV's movement and improve the UAV's obstacle avoidance efficiency:

$$\begin{cases}y_z(i)=\dfrac{1}{2N+1}[y(i+N)+y(i+N-1)+\cdots+y(i-N)]\\y_z(1)=y(1)\\y_z(2)=\dfrac{[y(1)+y(2)+y(3)]}{3}\\y_z(3)=\dfrac{[y(1)+y(2)+y(3)+y(4)+y(5)]}{5}\\y_z(4)=\dfrac{[y(2)+y(3)+y(4)+y(5)+y(6)]}{5}\end{cases}\tag{13}$$

The section line planning strategy in this chapter is formed based on the heuristic search algorithm, which is used to optimize the route smoothness while using a reasonable heuristic search algorithm and combining it with the jump point search to improve the overall performance of the path planning.

III. A. 2) Direction Selection Improvements

The direction of the combined gravitational force and repulsive force of the artificial potential field law is used as the reference direction of the RAPA algorithm. When the reference point and the current point direction are the same, the jump point is searched along the current point direction: if the two directions are different, the reference direction and the current point direction are searched in turn, which largely reduces the searching and storing of useless jump points, reduces the computation and memory occupancy problems for the RAPA algorithm, and improves the efficiency of the algorithm. The heuristic function can evaluate the advantage or cost of a node based on its characteristics and target information. The traditional gravitational and repulsive fields are usually defined as:

$$U_{att}(p) = 0.5\alpha \mid P_t - P \mid \tag{14}$$

$$F = F_{att} + F_{rep} \tag{15}$$

where P, P_t are the current point and target point position vectors, respectively. P_0 is the obstacle nearest position vector to the current node. ρ_0 is the influence distance of the obstacle repulsive field. α, β is the gravitational and repulsive positive proportionality gain coefficient, respectively. Since the search process of the hopping point search algorithm is usually parallelizable, the search task can be assigned to multiple computing units and searched simultaneously. Parallelized search can speed up the search and search more nodes in the same time with multiple processing units. Through rational task scheduling and result integration, the enabling resources can be fully utilized and the search efficiency can be improved. The gravitational force and repulsion are equal to the negative gradient of the gravitational and repulsive field functions, respectively, i.e., the force:

$$F_{att} = -\nabla U_{att} = \alpha \mid P_t - P \mid \tag{16}$$

And the virtual force on the current point is the vector sum of the two, so that Eq. (17) can be obtained:

$$F_{rep}(p) = -\nabla U_{rep} = \begin{cases} \beta\left(\dfrac{1}{\mid P_0 - P \mid} - \dfrac{1}{P_0}\right)\dfrac{1}{\mid P_0 - P \mid^2} & if \mid P_0 - P \mid < \rho \\ 0 & if \mid P_0 - P \mid \geq \rho_0 \end{cases} \tag{17}$$

The artificial potential field method plans the motion trajectory in an iterative manner, and the virtual force determines the direction of the next step. Starting from the starting point, every time a selected jump point is reached, the next step direction calculated by the artificial potential field method is used as the RAPA direction. Adopting the artificial potential field method to guide the direction can greatly reduce the amount of RAPA calculation and storage, which in turn improves the efficiency of path planning. According to specific needs and application scenarios, the improvement methods can be flexibly selected and combined to further optimize and refine the process of path planning.

III. A. 3) Adaptive parameter tuning

Adaptive parameter tuning is a technique used to improve algorithms with the potential to optimize search performance and adapt to the needs of different scenarios. In a jump-point search algorithm, parameters such as heuristic function weights and thresholds for pruning criteria can have a significant impact on the performance and effectiveness of the algorithm. By utilizing the adaptive parameter tuning technique, these parameters can be dynamically adjusted during the search process to adapt to different scenarios and requirements in path planning, thus making the algorithm more adaptive and robust.

III. B. Path tracking control methods

The design of the motion loop sliding mode control law and attitude loop sliding mode control law is discussed to ensure the accurate tracking of the pavement construction UAV to the desired path of the output of the improved artificial potential field method, and the control system structure is shown in Fig. 3.

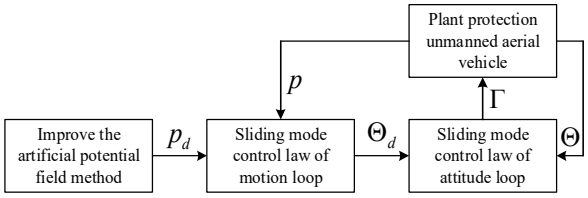

Figure 3: Control System Structure

III. B. 1) Motion Loop Control Law Design

Path tracking errors of road construction drones:

$$e_1 = p - p_d \tag{18}$$

where, p_d - the desired path of the output of the improved artificial potential field method, $p_d = [x_d, y_d, z_d]^T$.

In order to overcome the local minimum problem of the traditional artificial potential field method, the loop force is designed such that $e_2 = v + c_1 e_1 - \dot{p}_d$, where c_1 is the control parameter, which is a positive constant, and then the sliding mode plane for the design of the movement loop of the pavement construction UAV is:

$$S_1 = k_1 e_1 + e_2 = (k_1 + c_1) e_1 + \dot{e}_1 \tag{19}$$

where, k_1 - control parameter, a positive constant,

Consider the following Lyapunov function:

$$V_1 = \frac{1}{2} e_1^T e_1 + \frac{1}{2} S_1^T S_1 \tag{20}$$

Derivation of Eq. (20) yields:

$$\dot{V}_1 = e_1^T (v - \dot{p}_d) + S_1^T [(k_1 + c_1)\dot{e}_1 + \ddot{e}_1] \tag{21}$$

Substituting $e_2 = v + c_1 e_1 - \dot{\rho}_d$ and Eq. (6) into Eq. (21) and simplifying yields:

$$\dot{V}_1 = -c_1 e_1^T e_1 + e_1^T e_2 + S_1^T \left[(k_1 + c_1)\dot{e}_1 - G + hT + d_v - \ddot{p}_d\right] \tag{22}$$

Then the sliding mode control law for designing the pavement construction UAV motion loop is:

$$\begin{aligned} T = h^{-1}[&G - (k_1 + c_1)\dot{e}_1 + \ddot{p}_d - k_2 S_1 - \operatorname{sgn}(S_1) \\ &-(S_1^T)^{-1} e_1^T e_2 - D_v \operatorname{sgn}(S_1)] \end{aligned} \tag{23}$$

where, k_2 - control parameter, a positive constant, D_v - upper bound of the motion model perturbation term d_v.

Substituting Eq. (23) into Eq. (22), the simplification can be obtained:

$$\begin{aligned} &\dot{V}_1 = -c_1 e_1^T e_1 - k_2 S_1^T S_1 - |S_1^T| + (S_1^T d_v - |S_1^T| D_v) \le \\ &-c_1 e_1^T e_1 - k_2 S_1^T S_1 - |S_1^T| \le 0 \end{aligned} \tag{24}$$

Then, from Lyapunov stability theorem, it can be obtained that the sliding mode control law Eq. (23) can ensure the stability of the motion loop of the pavement construction UAV.

From the calculation of the sliding mode control law Eq. (23) and Eq. (2), the attitude command of the pavement construction UAV can be obtained as:

$$\begin{cases} \psi_d = \arctan \dfrac{y_d}{x_d} \\ \phi_d = \arcsin\left(\dfrac{T_x \sin\psi - T_y \cos\psi}{\sqrt{T_x^2 + T_y^2 + T_z^2}}\right) \\ \theta_d = \arctan\left(\dfrac{T_x \cos\psi + T_y \sin\psi}{T_z + mg}\right) \end{cases} \tag{25}$$

where, Θ_d - the UAV's attitude angle command, $\Theta_d = [\phi_d, \theta_d, \psi_d]^T$, ϕ_d, θ_d, ψ_d - roll angle command, pitch angle command and heading angle command.

III. B. 2) Attitude loop control law design

Attitude tracking errors of road construction UAVs:

$$e_3 = \Theta - \Theta_d \tag{26}$$

Let $e_4 = W\omega + c_2 e_3 - \dot{\Theta}_d$ where c_2 is the control parameter and is a positive constant, then the sliding mode surface for the design of the attitude loop of the pavement construction UAV is:

$$S_2 = k_3 e_3 + e_4 = (k_3 + c_2)e_3 + \dot{e}_3 \tag{27}$$

Consider the following Lyapunov function:

$$V_2 = \frac{1}{2} e_3^T e_3 + \frac{1}{2} S_2^T S_2 \tag{28}$$

$$\dot{V}_2 = e_3^T (W\omega - \dot{\Theta}_d) + S_2^T \left[(k_3 + c_2)\dot{e}_3 + \ddot{e}_3 \right] \tag{29}$$

where, k_3 - control parameter, a positive constant.

Substituting $e_4 = W\omega + c_2 e_3 - \dot{\Theta}_d$ and Eq. (7) in Eq. (29) yields:

$$\dot{V}_2 = -c_2 e_3^{ú} e_3 + e_3^{ú} e_4 + S_2^{ú} \left[(k_3 + c_2)e_3 + W(f + \Gamma + d_w) - \ddot{\Theta}_d \right] \tag{30}$$

where, k_4 - control parameter, a positive constant.

Derivation of Eq. (28) is obtained:

Then the sliding mode control law for designing the pavement construction UAV attitude loop is:

$$\begin{aligned} \Gamma = W^{-1}[& -Wf - (k_3 + c_2)\dot{e}_3 + \ddot{\Theta}_d - k_4 S_2 \\ & - \mathrm{sgn}(S_2) - (S_2^{ú})^{-1} e_3^{ú} e_4 - W D_* \,\mathrm{sgn}(S_2)] \end{aligned} \tag{31}$$

Substituting Eq. (31) into Eq. (30) and simplifying gives:

$$\begin{aligned} \dot{V}_2 = & -c_2 e_3^{ú} e_3 - k_3 S_2^{ú} S_2 - |S_2^{ú}| + (S_2^{ú} d_\omega - |S_2^{ú}| D_w) \le \\ & -c_2 e_3^{ú} e_3 - k_3 S_3^{ú} S_2 - |S_2^{ú}| \le 0 \end{aligned} \tag{32}$$

where, D_ω - the upper bound of the perturbation term d_ω of the attitude motion model.

Then, from the Lyapunov stability theorem, it can be obtained that the sliding mode control law Eq. (31) ensures that the attitude loop of the pavement construction UAV is stabilized.

IV. Simulation verification

In order to verify the validity of this scheme, the experiment is carried out in MatlabR2018a, the total simulation time is 300s, and the sampling time ΔT is 1s. The experimental field is of size 6km×6km, in which the obstacles are randomly generated, the inner circle is the forbidden area, and the outer circle is the influence area. Assuming that there are three UAVs collaboratively tracking a ground moving target, the starting position of the three UAVs is represented by a small airplane, and the starting and ending positions of the target are represented by triangles, to which seven obstacles with different sizes of the influence area are arbitrarily added, with an influence range of 200-400 m. Other parameters of the UAVs are: maximum speed 35 m/s, minimum speed 13 m/s, maximum acceleration 1m/s², maximum roll angle of 30°, and flight altitude of 1000 m. The simulation results are shown in Fig. 4.

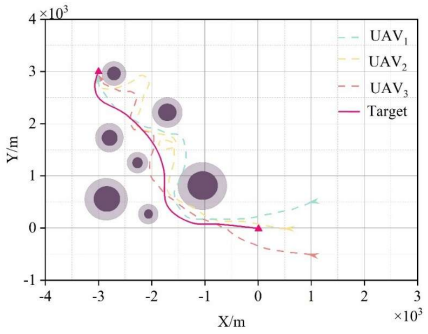

Figure 4: The drone coordinated target to track the barrier

In this case, the initial states of the UAV and the ground target are shown in Table 1.

Table 1: The initial state information of the drone and target

	Initial position/ (km, km)	Initial course/ (°)	Initial velocity/ (m/s)
Target	(0, 0)	90	15.3
UAV_1	(1, 0.5)	90	18
UAV_2	(0.5, 0)	90	18
UAV_3	(1, -0.5)	90	18

The obstacle location information and radius of influence are shown in Table 2.

Table 2: Obstacle location information and impact radius

Obstacle	Position/ (km, km)	Forbidden radius/km	Influence radius/km
1	(-2.81, 0.54)	0.2	0.4
2	(-2.51, 2.30)	0.1	0.2
3	(-2.21, 1.13)	0.2	0.4
4	(-1.91, 0.99)	0.1	0.2
5	(-1.61, 2.09)	0.15	0.3
6	(-1.31,1.44)	0.15	0.3
7	(-1.00, 0.79)	0.1	0.2

The relative distance between the UAV and the target is shown in Figure 5. The UAV tracking target distance fluctuates within a certain range and meets the tracking requirements.

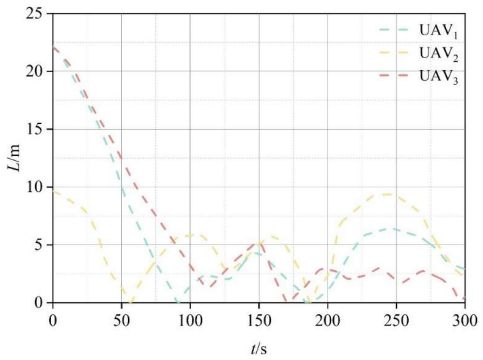

Figure 5: The relative distance of the drone and the target

The flight speed, flight acceleration, heading angle and roll angle of the UAV are shown in Fig. 6 to Fig. 9, respectively. The flight speed, acceleration, heading angle and roll angle satisfy the preset constraints.

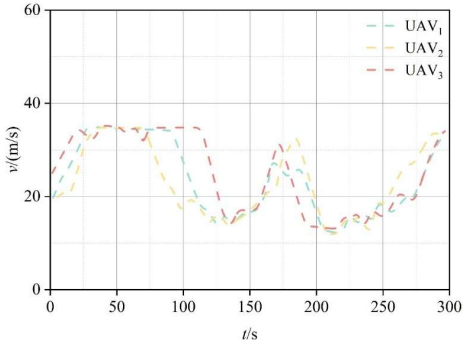

Figure 6: Flying speed of drones

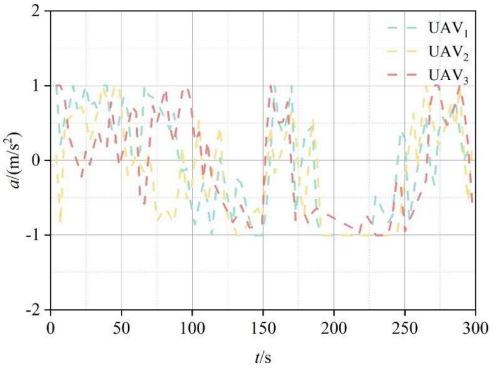

Figure 7: The flight acceleration of the drone

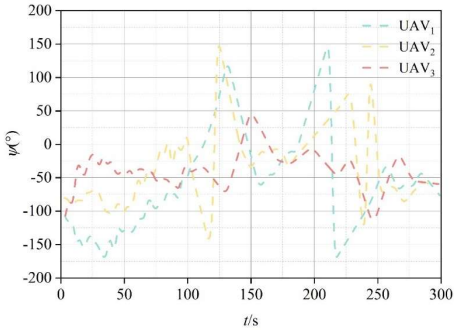

Figure 8: The course Angle of the drone

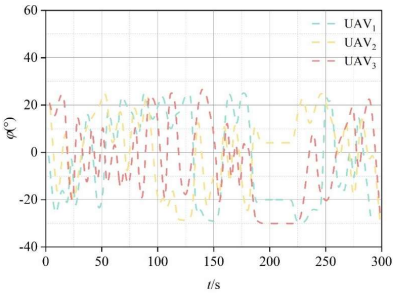

Figure 9: The drone's roll Angle

The distance between UAVs is shown in Figure 10. After the UAVs enter the cooperative state in 85s, the lower limit of the inter-aircraft collision avoidance distance is always satisfied, and the inter-aircraft communication distance is always greater than 0.2, which ensures that the UAVs can track the target within the safe collision avoidance range. It also fully meets the requirements of the upper limit of the inter-copter communication distance, and does not interrupt the communication between the UAVs, and has a large margin, which enables the timely exchange of the observed target information, making the prediction of the target more accurate, thus improving the tracking stability of the target.

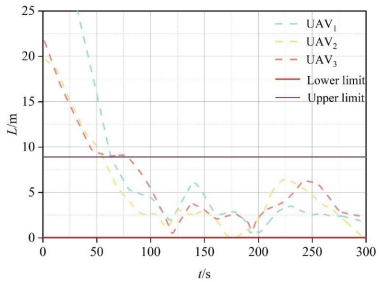

Figure 10: The distance between drones

The minimum and maximum distances between UAVs (after 85s) are shown in Table 3.The three UAVs can maintain a safe distance of more than 18m between each other, and can ensure that after entering the cooperative range, the UAVs can keep within 700m between each other, which is mutually verified with Fig. 10 to conclude that the cooperative performance of this path planning is flexible and efficient.

Table 3: The minimum distance between the drones and the maximum distance

	Minimum distance/m	Maximum distance/m
UAV1 and UAV2	18.63	679.63
UAV2 and UAV3	34.52	659.64
UAV3 and UAV1	45.11	620.58

The minimum distance between the UAVs and the obstacles is shown in Table 4.The three UAVs can maintain a safe distance of more than 100 m from all the obstacles and can fly away quickly after entering the influence area of the obstacles, which verifies that the obstacle avoidance performance derived from this path planning is safe and reliable.

Table 4: The minimum distance of a drone and an obstacle (m)

Obstacle	UAV1	UAV2	UAV3
1	438.25	167.89	455.35
2	239.35	173.92	107.64
3	406.05	127.34	330.88
4	371.07	574	323.75
5	296.51	265.17	221.03
6	145.76	216.74	350.09
7	408.6	489.82	461.64

V. Engineering applications

The pavement construction of a national highway in southwest China is taken as an example for application research. In order to satisfy the crushing operation of various dam materials in the construction process, a total of 15 crushers, including transition material crusher, stone stacker crusher and heart wall gravel soil, are installed with unmanned crusher on-board module at the project site, and an unmanned crusher fleet of unmanned crusher is constructed which is applied to the whole dam materials at the project site. At the same time, communication links and servers are arranged in the general control center to realize the two-way communication of the unmanned roller group, and the remote command module is set up to realize the real-time monitoring, task planning, and instruction issuance of the unmanned roller group.

Taking a certain moment of dam face crushing as an example, 8 sets of unmanned crushers are put into on-site production. Firstly, the construction manager sends the task to the system for the designated area. Secondly, the construction manager operating system inputs the operation parameters in the upstream rock pile area (Region 1), the heart wall area (Region 2) and the downstream transition area (Region 3) according to the operation tasks for the unmanned roller fleet to carry out the path planning, and the unmanned roller fleet cooperates with the full-coverage operation path as shown in Fig. 11. Then, the command system of the construction management personnel sends the operation instructions to each unmanned roller through the data link.

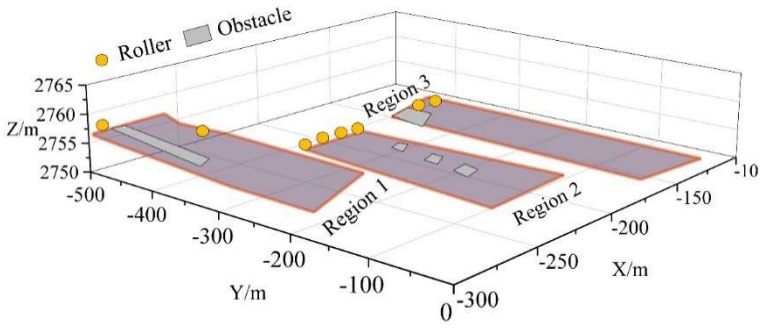

Figure 11: The unrolled group is fully covered by the work path

The process of unmanned milling machine group coordinated full-coverage operation is as follows:

(1) Each unmanned roller in each material area receives the corresponding task path.

(2) Each unmanned compactor carries out the operation according to the planned path in the respective task area. The upstream rock pile area and the downstream transition area are operated by the lap method, and the heart wall area is operated by the staggered spacing method.

(3) Each unmanned crusher completes the crushing operation and realizes the synergistic full coverage of the working surface of the upstream rock pile area, the heart wall area and the downstream transition area respectively. After the operation is completed, the construction manager generates quality and operation time reports through the system for acceptance.

In terms of milling quality, the graphical report of the number of passes generated by the system after analyzing the completion of the operation is shown in Figure 12. It was found that the compaction compliance rate of 94.36% on the face of the rock pile bin was greater than the standard value of 90%. The compaction compliance rate of 95.11% for the transition material bin face is greater than the standard value of 95%. For the heartwall gravel soil bin face, the compaction compliance rate of 96.62% is greater than the 95% standard value. The proposed path planning method can be realized to meet the needs of the milling process for milling multiple material areas on the dam face.

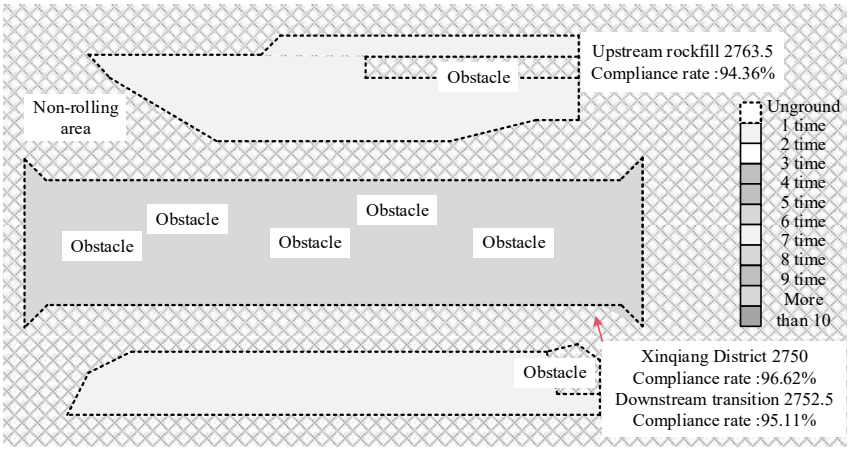

Figure 12: Report on the number of rolling passes

In terms of crushing efficiency, there is uncertainty in the speed control of unmanned mills, which makes it difficult to simultaneously fulfill the operation tasks assigned in equal amounts according to time and cost, and the final operation duration is shown in Figure 13. Among them, the average operation time of unmanned mills in the rock pile area, the heart wall area and the transition area accounted for 99.32%, 97.07% and 97.81% of the total time, respectively. The data show that the proposed group path planning method can equalize the operating time cost of each unmanned roller in the group, and the equipment utilization rate is high, which is conducive to improving the crushing efficiency under the condition of limited construction resources. The operational efficiency of the unmanned roller fleet can be further improved by optimizing the transverse and longitudinal control accuracy of the unmanned rollers.

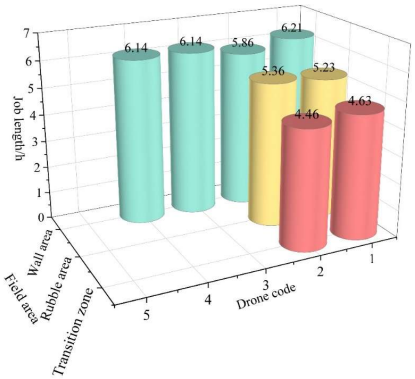

Figure 13: No one is counting the time of operation

VI. Study on safety and security in road construction by a fleet of unmanned aerial vehicles

VI. A. Optimization of UAV equipment

In the quality and safety management of highway engineering, the use of drone technology should be a good choice of drone application. Generally speaking, with the drone as the carrier, through carrying all kinds of sensors automation or intelligent way for data information collection, for engineering survey and design work to provide effective information support, can improve the overall management level [22]. If you want to give full play to the value of the drone, you need to comprehensively analyze the flight platform configuration and use and other aspects, and choose the appropriate drone equipment. At present, the commonly used types of UAVs include fixed-wing UAVs and unmanned helicopters as well as multi-rotor UAVs. Different drones have different advantages and characteristics, which need to be combined with economic analysis and application needs to do a comprehensive control, through comparative analysis to select the appropriate UAV equipment, to ensure that the entire operation can be carried out in an orderly manner. Divided according to the use, mainly including aerial photography drone and mapping drone and other types of drones, if divided according to the power system, it specifically includes battery or gasoline or oil-electric hybrid. In the practice of highway quality and safety management, surveying and mapping drones and aerial photography drones are mostly applied to grasp the environmental conditions of the highway construction site through comprehensive aerial photography of the entire highway beforehand, so as to provide strong support for the subsequent design and planning. Through the effective analysis of the collected data information, it provides strong support for the design quality control, and then realizes the prior control of the construction quality of the whole project. During the construction operation, the drone is used to carry out aerial photography inspection of the whole operation site to grasp the operation situation and provide corresponding data for quality and safety analysis.

VI. B. Good planning and design of aerial photography operations

The main form of application of drone technology in the practice of quality and safety management of highway construction is aerial photography. In order to ensure the effect of aerial photography, it is necessary to do a good job of planning and design. According to the needs of highway quality and safety management, a suitable route is formulated to guide the development and implementation of aerial photography operations. The preparation of the aerial photography operation plan is required to determine the aerial photography route and the basic configuration of aerial photography, such as camera models. The challenges and problems that may be encountered in the aerial photography operation need to be analyzed accordingly, and effective countermeasures and solutions need to be put forward to ensure that the entire aerial photography operation can be carried out in an orderly and high-quality manner, and that complete data and information can be collected to provide support for the subsequent quality control and safety management.

VI. C. Make good use of the results of aerial photography

If you want to effectively play the value of the application of UAV technology, you must do a good job in the use of aerial photography results, according to the management requirements and specifications of the site, combined with the data information collected from aerial photography, to provide corresponding data for the quality management and safety management staff, so that they can be in accordance with the collection of the video or data information obtained by the quality of the management and safety management optimization, to ensure that the entire production work of the site has been effectively controlled. Effective control.

VI. D. Enhanced integration of technology with other tools

With the application and development of intelligent technology, more and more intelligent technical means are widely used in engineering quality and safety management practice, such as intelligent chemical site management system. The effective integration of drone technology and other technologies can lead to the improvement and optimization of the value of technical application and provide strong support for the development of related work. It is necessary to do a good job of effective cooperation between various departments, jointly provide technical support and guarantee for quality management and safety control, ensure that the whole operation is comprehensively and effectively controlled, and discover the problems and deficiencies in a timely manner. Explore the advantages and shortcomings of the application of GIS technology and video surveillance technology, seek the key points of the combined use of technology, and develop the corresponding quality and safety management system, so as to promote the high quality of the work can be carried out and implemented.

VII. Conclusion

The study is based on the improved RAPA path planning algorithm and path tracking control method to realize the effective construction of unmanned aircraft swarm on highway pavement. In the simulation test, three UAVs can continuously track the target effectively and keep a safe distance of more than 100 m from all obstacles.The results of the application of eight pavement construction UAV fleets in the pavement construction of a national highway in Southwest China show that this paper's scheme can quickly and accurately plan smooth obstacle-avoiding construction paths, and the designed sliding mode path control method can ensure that the pavement construction UAV fleet can accurately track the obstacle-avoiding construction paths. The UAV formation can accurately track the obstacle avoidance construction path, and this paper's program has effectiveness and feasibility in highway pavement operation, which has important application value. Finally, in the aspects of UAV equipment, aerial photography operation planning and design, and aerial photography results utilization, further proposed to protect the safety measures of UAV in the construction process.

References

[1] Floros, G. S., & Ellul, C. (2021). LOSS of INFORMATION during design & construction for highways asset management: A GeoBIM perspective. ISPRS annals of the photogrammetry, remote sensing and spatial information sciences, 8, 83-90.

[2] Xu, X., Yuan, C., Zhang, Y., Cai, H., Abraham, D. M., & Bowman, M. D. (2019). Ontology-based knowledge management system for digital highway construction inspection. Transportation Research Record, 2673(1), 52-65.

[3] Deep, S., Banerjee, S., Dixit, S., & Vatin, N. I. (2022). Critical factors influencing the performance of highway projects: an empirical evaluation. Buildings, 12(6), 849.

[4] Moghayedi, A., & Windapo, A. (2019). Key uncertainty events impacting on the completion time of highway construction projects. Frontiers of Engineering Management, 6(2), 275-298.

[5] Mohamed, M., & Tran, D. Q. (2023). Exploring the relationships between project complexity and quality management approaches in highway construction projects. Transportation Research Record, 2677(5), 390-402.

[6] Radzi, A. R., Rahman, R. A., & Doh, S. I. (2023). Decision making in highway construction: A systematic review and future directions. Journal of engineering, design and technology, 21(4), 1083-1106.

[7] Wu, X., Zhao, W., Ma, T., & Yang, Z. (2019). Improving the efficiency of highway construction project management using lean management. Sustainability, 11(13), 3646.

[8] Shi, Z. (2020, October). Research on Innovation Management of Highway Construction Project Based on Big Data. In Journal of Physics: Conference Series (Vol. 1648, No. 4, p. 042036). IOP Publishing.

[9] Zhou, Z., Irizarry, J., & Lu, Y. (2018). A multidimensional framework for unmanned aerial system applications in construction project management. Journal of Management in Engineering, 34(3), 04018004.

[10] Amoah, R. (2022). Application of Project Time Management and Resource Management to a Novel Blended Wing Unmanned Aerial Vehicle (BWB UAV) Design. Open Access Library Journal, 9(9), 1-23.

[11] Ersoz, A. B., Pekcan, O. N. U. R., & Tokdemir, O. B. (2019). Lean project management using unmanned aerial vehicles. Tamap J. of Engineering, 65.

[12] Li, Y., Gao, S., Liu, X., Zuo, P., & Li, H. (2023). An efficient path planning method for the unmanned aerial vehicle in highway inspection scenarios. Electronics, 12(20), 4200.

[13] Outay, F., Mengash, H. A., & Adnan, M. (2020). Applications of unmanned aerial vehicle (UAV) in road safety, traffic and highway infrastructure management: Recent advances and challenges. Transportation research part A: policy and practice, 141, 116-129.

[14] Barrile, V. I. N. C. E. N. Z. O., Bernardo, E., Fotia, A., Candela, G. A. B. R. I. E. L. E., & Bilotta, G. (2020). Road safety: road degradation survey through images by UAV. WSEAS Transactions on Environment and Development, 16, 649-659.

[15] Jiang, X., Cui, Q., Wang, C., Wang, F., Zhao, Y., Hou, Y., ... & Shi, G. (2023). A model for infrastructure detection along highways based on remote sensing images from UAVs. Sensors, 23(8), 3847.

[16] Feitosa, I., Santos, B., & Almeida, P. G. (2024). Pavement inspection in transport infrastructures using unmanned aerial vehicles (UAVs). Sustainability, 16(5), 2207.

[17] Pan, Y., Chen, X., Sun, Q., & Zhang, X. (2021). Monitoring asphalt pavement aging and damage conditions from low-altitude UAV imagery based on a CNN approach. Canadian Journal of Remote Sensing, 47(3), 432-449.

[18] Fang, Z., & Savkin, A. V. (2024). Strategies for optimized uav surveillance in various tasks and scenarios: A review. Drones, 8(5), 193.

[19] Chen Yafei & Deng Tao. (2023). Leader-Follower UAV formation flight control based on feature modelling. Systems Science & Control Engineering,11(1),

[20] Chen Tao,Chen Suifan,Zhang Kuoran,Qiu Guoting,Li Qipeng & Chen Xinmin. (2022). A jump point search improved ant colony hybrid optimization algorithm for path planning of mobile robot. International Journal of Advanced Robotic Systems,19(5),

[21] Yijun Huang,Hao Li,Yi Dai,Gehao Lu & Minglei Duan. (2024). A 3D Path Planning Algorithm for UAVs Based on an Improved Artificial Potential Field and Bidirectional RRT*. Drones,8(12),760-760.

[22] Zhu Chendong,Zhu Junqing,Bu Tianxiang & Gao Xiaofei. (2022). Monitoring and Identification of Road Construction Safety Factors via UAV. Sensors,22(22),8797-8797.